RESEARCH ARTICLE

WILEY

Roughness effect on the correction factor of surface velocity for rill flows

Alessio Nicosia[1] [ORCID] | Costanza Di Stefano[1] | Vincenzo Palmeri[2] [ORCID] |
Vincenzo Pampalone[1] [ORCID] | Vito Ferro[2] [ORCID]

[1]Department of Agricultural, Food and Forestry Sciences, University of Palermo, Viale delle Scienze, Palermo, Italy

[2]Department of Earth and Marine Sciences, University of Palermo, Palermo, Italy

Correspondence
Alessio Nicosia, Department of Agricultural, Food and Forestry Sciences, University of Palermo, Viale delle Scienze, Building 4, 90128 Palermo, Italy.
Email: alessio.nicosia@unipa.it

Abstract

Flow velocity is one of the most important hydrodynamic variables for both channelized (rill and gullies) and interrill erosive phenomena. The dye tracer technique to measure surface flow velocity V_s is based on the measurement of the travel time of a tracer needed to cover a known distance. The measured V_s must be corrected to obtain the mean flow velocity V using a factor $\alpha_v = V/V_s$ which is generally empirically deduced. The V_s measurement can be influenced by the method applied to time the travel of the dye-tracer and α_v can vary in different flow conditions. Experiments were performed by a fixed bed small flume simulating a rill channel for two roughness conditions (sieved soil, gravel). The comparison between a chronometer-based (CB) and video-based (VB) technique to measure V_s was carried out. For each slope-discharge combination, 20 measurements of V_s, characterized by a sample mean V_m, were carried out. For both techniques, the frequency distributions of V_s/V_m resulted independent of slope and discharge. For a given technique, all measurements resulted normally distributed, with a mean equal to one, and featured by a low variability. Therefore, V_m was considered representative of surface flow velocity. Regardless of roughness, the V_m values obtained by the two techniques were very close and characterized by a good measurement precision. The developed analysis on α_v highlighted that it is not correlated with Reynolds number for turbulent flow regime. Moreover, α_v is correlated neither with the Froude number nor with channel slope. However, the analysis of the empirical frequency distributions of the correction factor demonstrated a slope effect. For each technique (CB, VB)-roughness (soil, gravel) combination, a constant correction factor was statistically representative even if resulted in less accurate V estimations compared to those yielded by the slope-specific correction factor.

KEYWORDS
correction factor, dye method, flow velocity, interrill flows, rill flows, soil erosion

1 | INTRODUCTION

Flow velocity is one of the most important hydrodynamic variables controlling channelized (rill and gully) and interrill erosion processes and process-based soil erosion models can be developed and tested by its knowledge and measurement (Takken et al., 1998).

Among the numerous methods (hot film anemometry, Particle Imaging Velocimetry-PIV, Acoustic Doppler Velocimetry-ADV, infrared thermography, optical tacheometer) (Ali et al., 2012; Ayala et al., 2000; de Lima & Abrantes, 2014; Dunkerley, 2003; Giménez et al., 2004; Raffel et al., 1998) developed to measure flow velocity in interrill and rill flows, the dye-tracer technique (Ban et al., 2016; Bradley et al., 2002; Lei et al., 2005; Zhang et al., 2010) is still one of the most applied for overland (Dunkerley, 2001; Novak et al., 2017; Polyakov et al., 2021) and rill flows (Abrahams et al., 1996; Bagarello et al., 2015; Bruno et al., 2008; Di Stefano et al., 2015; Di Stefano et al., 2017a; Foster et al., 1984; Gilley et al., 1990; Govers, 1992; Line & Meyer, 1988). Probably, the reason for the wide spread of this technique is its simplicity (Wirtz et al., 2010, 2012) while other methods, as hot film anemometry, ADV and PIV, are more sophisticated, useful for laboratory investigations (Ali et al., 2012) and can be negatively affected by sediment transport, low flow depths and not-controlled conditions occurring in the field (Liu et al., 2001; Planchon et al., 2005).

This technique is based on the measurement of the travel time of a tracer (water marker, salt, magnetic material, water isotope) (Berman et al., 2009; Dunkerley, 2003; Olivier et al., 2005; Ventura Jr. et al., 2001) needed to cover the known distance from the injection point (Chen et al., 2017) to a given section. This measured surface flow velocity V_s must be corrected with a correction factor α_v to obtain the mean flow velocity V (Zhang et al., 2010):

$$\alpha_v = \frac{V}{V_s} \tag{1}$$

Indeed, for open channel flows local velocity varies along the vertical, is equal to zero at the bed and reach the maximum value at or below the water surface, depending on whether the effect of channel walls is negligible or not, respectively (Ferro & Baiamonte, 1994). The correction factor depends upon the form of the vertical velocity profile. For a laminar flow on a smooth surface the parabolical velocity profile can be determined theoretically (Powell, 2014). The presence of roughness elements can modify the shape of the vertical velocity profile (Ferro, 2003; Powell, 2014). Accordingly, a good accuracy of the mean flow velocity measurement should be achieved by setting an appropriate correction factor α_v for different hydraulic conditions.

Many investigations have been carried out exploring different conditions and determining different correction factor values. Horton et al. (1934) suggested $\alpha_v = 0.67$ for an infinitely wide laminar flow on a smooth and rigid bed. For transitional flows, Emmett (1970), carrying out flume experiments, found that α_v increases with flow Reynolds number $Re = Vh/\nu_k$, in which h is the water depth and ν_k is the kinematic viscosity, and α_v is equal to 0.8 for turbulent flow.

Luk and Merz (1992) determined experimentally an α_v value equal to 0.75 for transitional and turbulent flow. Li et al. (1996), carrying out flume experiments with transitional and turbulent flows on a mobile sand bed having a slope s ranging from 4.7% to 17.7%, empirically determined an inverse relationship of α_v with s (Li & Abrahams, 1997) and a direct relationship of α_v with Re.

For sediment-free overland flows, Li and Abrahams (1997) found that for laminar flows α_v decreases with the roughness height, increases rapidly with Re for transitional regime and more slowly with Re for turbulent flows, and is not affected by slope. For a sediment-free flow, Zhang et al. (2010) empirically established a relationship between the correction factor, slope and flow Reynolds number. Pan et al. (2015) carried out experimental runs with different roughness conditions and found α_v values almost equal to 0.8 for turbulent flows.

For sediment-laden flows, an inverse relationship between the correction factor and the sediment load was obtained by Li and Abrahams (1997) and Zhang et al. (2010). Ali et al. (2012), carrying out experiments in a mobile bed flume, established that the correction factor α_v increases as the size of the transported particles increases. Di Stefano et al. (2018b), using measurements of surface flow velocity (Di Stefano et al., 2017b, 2018a, 2018b) in rills incised on plots having a mean slope equal to 9, 14 and 22%, found that, to estimate the Darcy-Weisbach friction factor, α_v can be indifferently assumed equal to 0.665 or 0.80. Di Stefano et al. (2020) proposed a theoretical relationship, based on the power velocity distribution, to estimate α_v which was tested with flume measurements for sediment-free flow on a rough bed (Ferro & Baiamonte, 1994) and sediment-laden flow on a smooth bed (Coleman, 1986). The authors stated that the correction factor increases with the roughness height for the sediment-free flow while an inverse relationship between α_v and the sediment load can be established for the sediment-laden flow.

Chen et al. (2017) conducted experiments on sloping (5°, 10°, 15° and 20°) flumes 10 cm - wide, filled with black soil, to measure surface flow velocity over frozen and non-frozen slopes using the dye tracer method. They stated that rill flow velocity can be effectively measured with the latter by multiplying the surface velocity with a correction factor of 0.80.

Yang et al. (2020) carried out a laboratory investigation to study the effects of rill morphology and hydraulic characteristics on α_v for flume conditions with and without (rill-free) rills. In this investigation, the slope gradients varied from 5° to 25° and Reynolds numbers from 172 to 1040. The results showed that the α values obtained for rill-free flow and rill flow ranged from 0.295 to 0.729 and from 0.330 to 0.990, respectively. For the rill-free flows, Yang et al. (2020) stated that α_v is affected by the slope gradient and Reynolds number, while for rill flows α_v can be estimated by the rill depth and Reynolds number.

Polyakov et al. (2021), carrying out several experiments on overland flows in semiarid rangelands, suggested that the velocity correction factor is a dynamic, site specific property. These authors proposed a linear model to estimate the correction factor based on

predictor variables as travel distance, unit discharge, and surface velocity.

The available literature findings corroborate the idea that establishing an appropriate α_v value for correcting the surface velocity is a significant achievement to study rill flow hydraulics.

Since most of the available investigations regarding the correction factor were carried out for flume and overland flow, there is a scientific need to widen the existing knowledge (Chen et al., 2017; Yang et al., 2020) for rill flow scale.

Di Stefano et al. (2021) carried out an experimental investigation using a small flume with fixed smooth bed and walls, slope values ranging from 0.1% to 8.7% and clear discharge ranging from 0.3 to 0.87 L s^{-1}. These authors compared a chronometer-based (CB) and video-based (VB) technique to measure the travel time of the tracer. Each experimental run was characterized by a sample of 20 measurements of surface velocity V_s having a mean value V_m and was carried out with fixed values of slope and discharge. The empirical frequency distribution of the V_s/V_m ratio of the VB was more uniform than that of the CB technique. In any case, the sample mean V_m was representative of surface flow velocity for both techniques and the value obtained by the CB measurements lightly underestimated (-1.7%) that obtained by the VB technique. Di Stefano et al. (2021) also demonstrated that the correction factor is independent of flow Reynolds number while two relationships with a Froude number F_s related to surface velocity measurement and channel slope were established. The measurements by Di Stefano et al. (2021) were performed in a basic rill scheme, i.e., with a smooth bed and sediment free flow, that differs from that generally occurring in natural hillslopes but is a reference condition to study further effects (grain roughness, sediment transport) on the correction factor of the surface velocity. The effect of grain roughness is due to variation in flow velocity profile compared to the smooth bed case and, assuming as reference condition that investigated by Di Stefano et al. (2021), can be studied by experiments with sediment free flows. In this investigation experiments were performed with clear water flowing over a fixed rough bed in a flume simulating a rill in order to (i) compare, for two different roughness conditions, the measurements of surface flow velocity carried out by the CB and the VB techniques, (ii) test the effect of Froude number, Reynolds number and bed slope on the correction factor; and (iii) compare the results with those obtained in the same rill channel for a hydraulically smooth bed.

2 | MATERIALS AND METHODS

The experimental investigation was carried out using a sloping flume (5 m long, 0.078 m wide and 0.04 m high) located at the experimental area of the Department of Agriculture, Food and Forest Sciences of University of Palermo. The setup is the same used by Di Stefano et al. (2021).

Water entered the aluminium flume by a small pipe and an inflow device with wire meshes useful to allow the flow to span the entire flume width and dissipate flow turbulence. From the end section of the flume the flow was conveyed towards a downstream tank.

Experimental runs were carried out using two different roughness conditions. The first arrangement was obtained fixing, by a waterproof vinylic glue, a sieved soil (Figure 1) to the flume bed and walls. Figure 2 shows the particle size distribution of the investigated soil. The median diameter d_{50} of the soil was equal to 0.014 mm.

The second arrangement was obtained fixing, by a waterproof vinylic glue, gravel (Figure 3) to the flume bed and walls. To characterize the gravel elements, three diameters (d_1, d_2, d_3) (Figure 4) were measured using callipers. The diameters d_1 and d_2, measured on the same plane, represent the largest and the intermediate diameter, respectively, while d_3, perpendicular to d_1 and d_2, is the smallest one. The mean value, d_m, of these three measurements was considered the representative diameter of the gravel element. Figure 5 shows the empirical frequency distribution of the sample constituted by 100 d_m values. The median diameter d_{50} was equal to 4.7 mm.

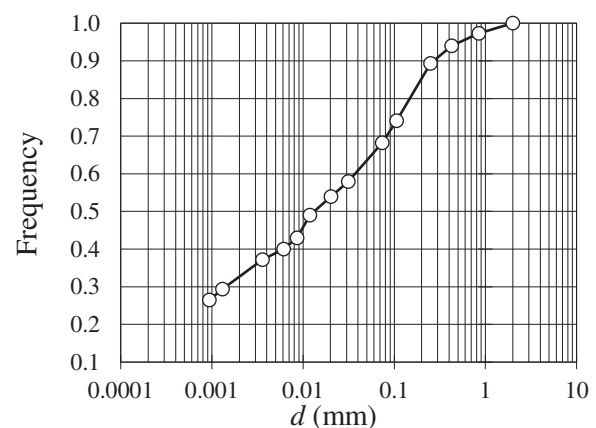**FIGURE 1** View of the flume covered by glued sieved soil

FIGURE 2 Particle size distribution of the investigated soil

FIGURE 3 View of the flume covered by glued gravel

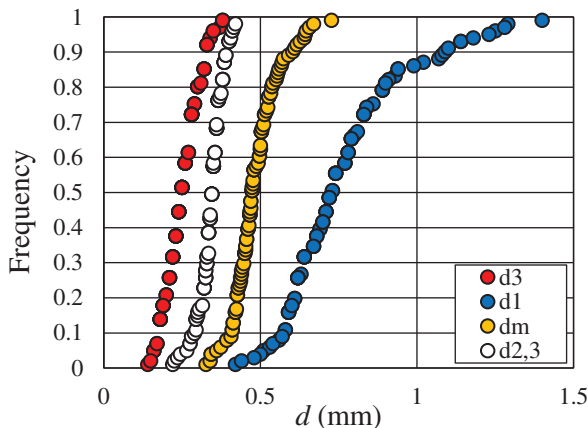**FIGURE 4** View of the measured largest (d_1) and intermediate (d_2) diameter of the gravel element

FIGURE 5 Cumulative empirical frequency distribution of d_1, d_{2-3}, d_3, d_m for the gravel arrangement

For both arrangements, the measurements were performed for six slope values s (0.1, 1.0, 2.5, 4.4, 6.1 and 8.7%). For each slope, four (for soil arrangement) and five (for gravel arrangement) values of discharge Q (from 0.21 to 0.907 L s^{-1}, Tables 1 and 2), were used.

TABLE 1 Characteristic data of the experimental runs carried out for flume covered with sieved soil

Q	s	h	Re	F
L s^{-1}	**%**	**m**	**—**	**—**
0.21	0.1	0.015	2400	0.46
0.36	0.1	0.019	4154	0.56
0.44	0.1	0.021	5078	0.58
0.65	0.1	0.027	7501	0.60
0.23	1.0	0.009	2654	1.10
0.36	1.0	0.014	4154	0.91
0.56	1.0	0.018	6462	0.93
0.66	1.0	0.019	7616	1.01
0.28	2.5	0.011	3197	0.98
0.45	2.5	0.015	5193	1.02
0.56	2.5	0.016	6462	1.11
0.70	2.5	0.019	8078	1.12
0.19	4.4	0.009	2193	0.96
0.39	4.4	0.012	4501	1.18
0.59	4.4	0.014	6809	1.43
0.72	4.4	0.016	8309	1.42
0.21	6.1	0.007	2400	1.55
0.36	6.1	0.010	4143	1.49
0.49	6.1	0.012	5655	1.61
0.76	6.1	0.014	8770	1.84
0.26	8.7	0.008	3035	1.56
0.49	8.7	0.010	5655	1.98
0.65	8.7	0.012	7501	2.08
0.76	8.7	0.014	8770	1.94

Therefore, each run was characterized by fixed values of slope s, discharge Q and water depth h (Tables 1 and 2). Discharge was measured by the volumetric technique and the water depth h_m was measured from the aluminium bed of the flume by a point gauge, having a measurement accuracy of ±0.1 mm, located in the flume axis at 2 m from the inlet section.

For each run, the flow cross-section area was calculated using the flow depth h, and the mean flow velocity V was calculated as the ratio between Q and the flow cross-section area. The Froude number F of the flow was calculated as $F = V/(g\,h)^{0.5}$, where g is gravitational acceleration.
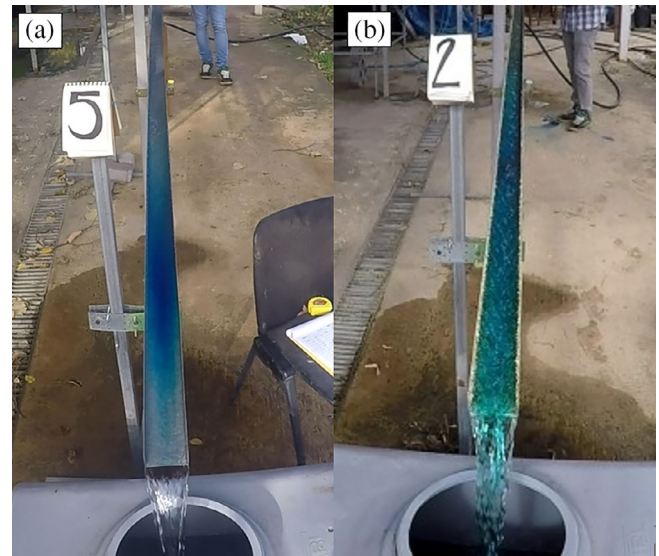
For the soil arrangement h was set equal to h_m while for the gravel arrangement the calculation of the actual flow cross-section area required to consider that the gravel glued to the flume bed and walls reduced flow width and depth as compared to the values measured from the aluminium flume. For this reason, the water depth h was referred to a reference plane coincident with that passing through the top of the elements characterized by a height equal to $d_{2,3-50}$ (3.5 mm) (Figure 5), which is the median value of the diameters $d_{2,3}$ calculated averaging the values of the intermediate (d_2) and the

TABLE 2 Characteristic data of the experimental runs carried out for flume covered with gravel

Q	s	h	Re	F
L s^{-1}	%	m	—	—
0.214	0.1	0.020	2713	0.35
0.305	0.1	0.025	3867	0.36
0.408	0.1	0.029	5173	0.38
0.470	0.1	0.031	5959	0.39
0.540	0.1	0.033	6846	0.40
0.336	1.0	0.015	4260	0.86
0.458	1.0	0.018	5806	0.85
0.520	1.0	0.018	6592	0.93
0.591	1.0	0.022	7493	0.84
0.662	1.0	0.022	8393	0.88
0.336	2.5	0.013	4260	1.07
0.480	2.5	0.015	6085	1.14
0.550	2.5	0.016	6973	1.17
0.622	2.5	0.017	7886	1.21
0.723	2.5	0.019	9166	1.22
0.397	4.4	0.012	5033	1.36
0.540	4.4	0.014	6846	1.39
0.622	4.4	0.015	7886	1.53
0.713	4.4	0.016	9039	1.65
0.825	4.4	0.017	10 459	1.63
0.367	6.1	0.009	4653	1.97
0.530	6.1	0.013	6719	1.60
0.642	6.1	0.014	8139	1.75
0.713	6.1	0.015	9039	1.79
0.846	6.1	0.016	10 725	1.80
0.387	8.7	0.012	4906	1.27
0.530	8.7	0.014	6719	1.43
0.632	8.7	0.014	8012	1.64
0.754	8.7	0.015	9559	1.90
0.907	8.7	0.018	11 499	1.66

FIGURE 6 Dye tracer technique applied for smooth flume (a) and flume covered by gravel (b)

technique is based on dye visual observation. The VB technique is based on the video-analysis by the free software Kinovea (www.kinovea.org) of the whole run (temporal resolution of 60 frames per second) recorded by a camera located downstream of the channel to identify the time of the tracer injection and that of the tracer arrival at the end of the flume.

For each run, the measurement of V_s was repeated 20 times and 20 values of the correction factor $\alpha_v = V/V_s$ were calculated. For a given run, the single mean value (i.e., the mean of the 20 measurements) of the surface velocity, V_m, the corresponding correction factor $\alpha_v = V/V_m$ and a particular Froude number F_s

$$F_s = V_m / \sqrt{gh} \qquad (2)$$

were also calculated. This last hydraulic variable was used to test the reliability of the relationship between α_v ($=V/V_m$) and F_s, which would allow to estimate the correction factor by the measured surface velocity.

For each slope s, the mean value of $\alpha_v = V/V_m$, corresponding to different discharges, named α_{vm}, was finally obtained.

For the soil and gravel arrangements and for each measurement technique, 480 and 600 measurements were carried out, respectively.

3 | RESULTS

3.1 | Comparison between VB and CB technique for measuring flow surface velocity

For the VB technique, Figure 7a (soil) and Figure 7b (gravel) show, as an example for $s = 1\%$, the empirical cumulative frequency distributions of the V_s/V_m ratio corresponding to the investigated discharges.
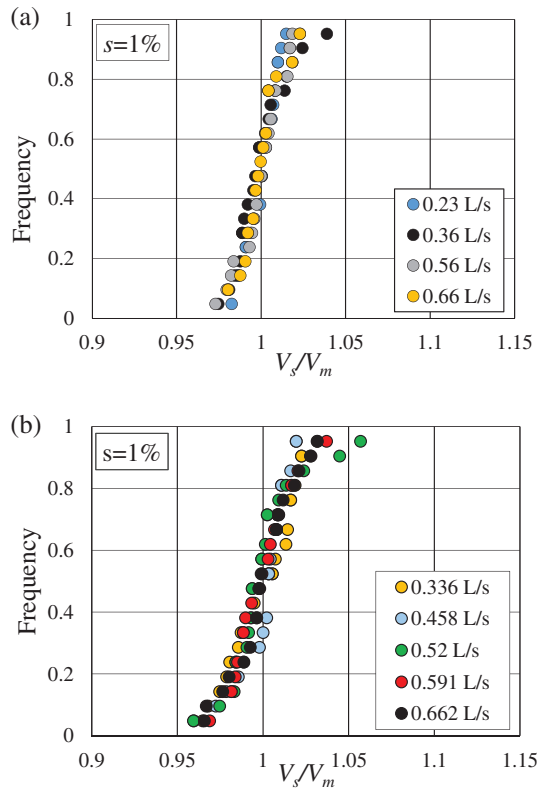
smallest (d_3) diameter of each sample element. In other words, for the gravel configuration the actual water depth h was equal to $h_m - d_{2,3-50}$ and the actual width of the flow cross-section was equal to $w - 2d_{2,3-50}$, in which w is the flume width. The choice of the $d_{2,3-50}$ is due to the circumstance that the gravel elements placed randomly to cover the flume surface tended to arrange themselves with the smallest or intermediate dimension perpendicular to the flume bed and walls.

A Methylene blue solution was used as a dye-tracer to measure the surface velocity V_s (Figure 6a,b). To avoid changes of the water properties, a small volume (2 mL) of the liquid marker was applied by a pipette. The tracer injection section was placed 4.3 m upstream from the end of the flume. The travel time of the leading edge of the dye cloud was measured using two different techniques. The CB

FIGURE 7 (a) Example of empirical cumulative frequency distributions of the V_s/V_m ratio corresponding to the investigated discharges for VB-soil combination. (b) Example of empirical cumulative frequency distributions of the V_s/V_m ratio corresponding to the investigated discharges for VB-gravel combination

FIGURE 8 (a) Example of empirical cumulative frequency distributions of the V_s/V_m ratio corresponding to the investigated discharges for CB-soil combination. (b) Example of empirical cumulative frequency distributions of the V_s/V_m ratio corresponding to the investigated discharges for CB-gravel combination

Each empirical frequency distribution refers to a sample of 20 measurements of V_s, carried out in the same experimental condition (fixed values of slope and discharge), having a mean value V_m. For the CB technique, Figure 8a (soil) and Figure 8b (gravel) show, as an example for the forementioned slope, the empirical cumulative frequency distributions of the V_s/V_m ratio for each discharge.

Figures 7 and 8 show that the distribution of the variable V_s/V_m can be considered independent of discharge. This result was confirmed by the Kolmogorov–Smirnov (KS) test (Kirkman, 1996). This test, which was used to statistically compare each pair of distributions, considers the maximum vertical deviation between two cumulative empirical distributions and the null hypothesis of no differences between data sets is rejected if the calculated P value is small (Kirkman, 1996; $P < 0.05$ in this investigation). For each roughness condition, the V_s/V_m values were used to plot the empirical distribution for fixed slope (Figure 9). For both the investigated rough beds, the overlapping of the six empirical frequency distributions for both the applied techniques (VB and CB) and the results of the KS test suggested that V_s/V_m does not depend on slope. Since the V_s/V_m ratio was independent of slope and discharge, the sample corresponding to a fixed roughness belongs to a single population. For this reason, a single frequency distribution of the V_s/V_m ratio for each measurement technique was considered. Figure 10 shows, as an example for the VB technique and the soil arrangement
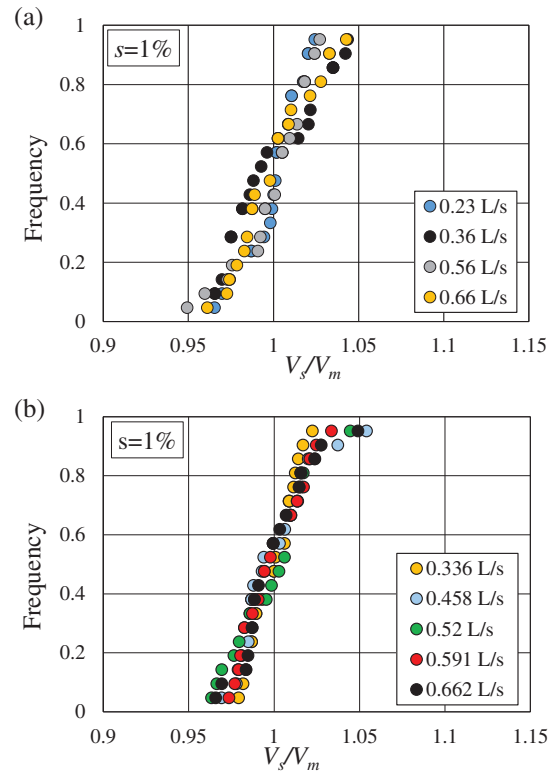
(Figure 10a) and the gravel one (Figure 10b), the frequency distribution of V_s/V_m. This figure also shows the normal distribution, with mean value of V_s/V_m equal to 1, having standard deviation equal to 0.012 (VB) and 0.016 (CB) for $d_{50} = 0.014$ mm, and 0.011 (VB) and 0.014 (CB) for $d_{50} = 4.7$ mm. Furthermore, each distribution is sub-vertical and characterized by V_s/V_m values close to 1 demonstrating that the mean value V_m can be considered representative of the flow velocity for each experimental run.

In Figure 11, for each $s - Q$ combination investigated here (Figure 11b,c) and by Di Stefano et al. (2021) ($d_{50} = 0$) (Figure 11a), the comparison between the V_m values determined by VB and CB techniques is plotted. For all the three cases, this figure shows a linear relationship between the two variables expressed by the following equations:

$$V_{mVB} = 1.016 V_{mCB} \qquad \text{for } d_{50} = 0 \tag{3}$$

$$V_{mVB} = 1.013 V_{mCB} \qquad \text{for } d_{50} = 0.014 \text{ mm} \tag{4}$$

$$V_{mVB} = 1.033 V_{mCB} \qquad \text{for } d_{50} = 4.7 \text{ mm} \tag{5}$$

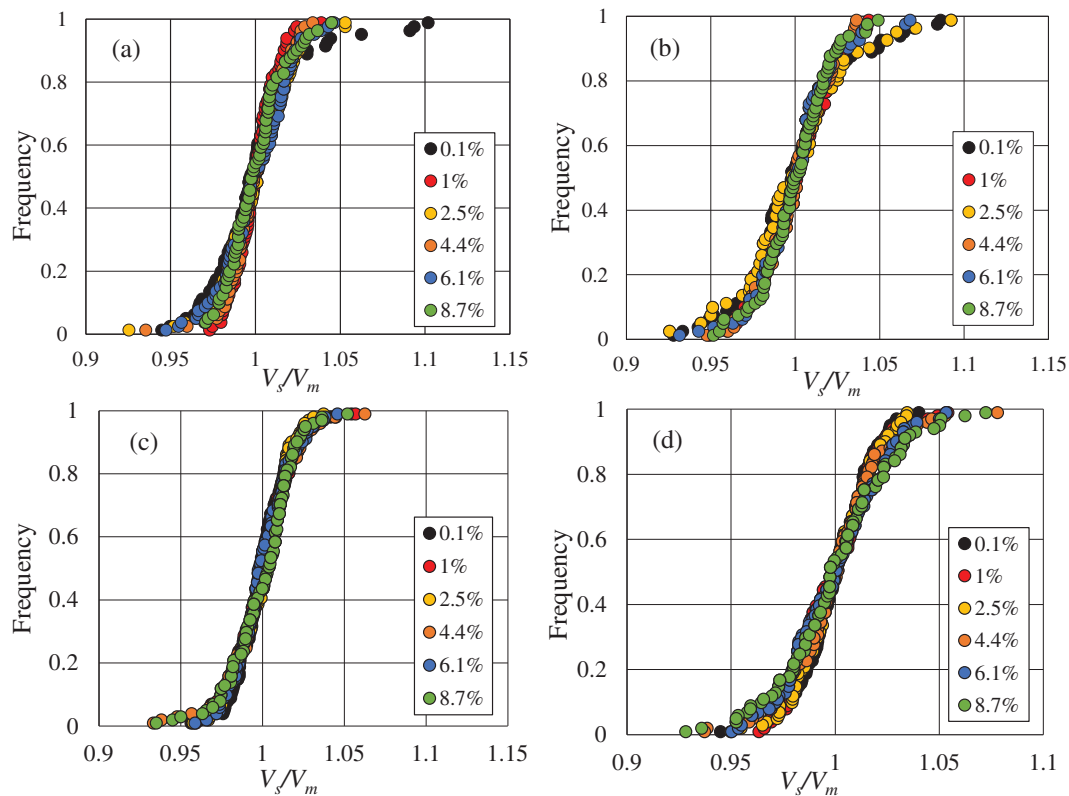that are all characterized by a coefficient of determination greater than 0.99.

FIGURE 9 Empirical cumulative frequency distributions of the V_s/V_m ratio corresponding to the investigated slopes for VB-soil (a), CB-soil (b), VB-gravel (c) and CB-gravel (d) combinations
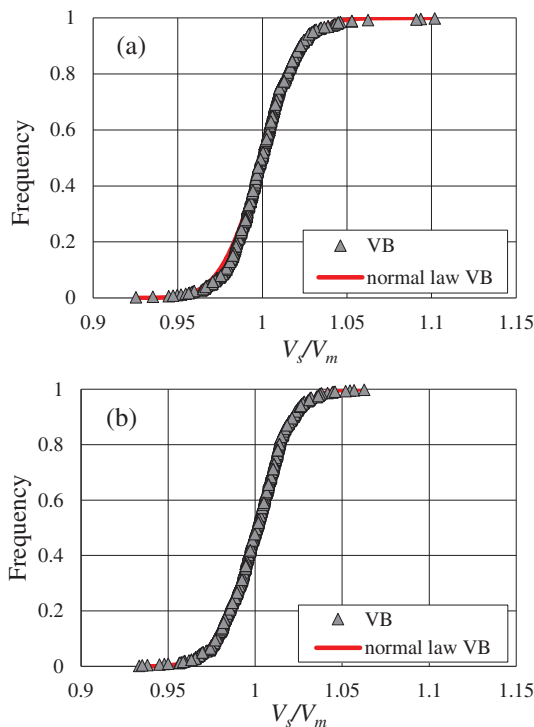

FIGURE 10 Empirical cumulative frequency distributions of the V_s/V_m ratio, as an example for VB-soil (a) and VB-gravel (b) combinations

For analysing the variability of the surface velocity V_s for the two applied techniques and roughness conditions, for each experimental run the coefficient of variation $CV(V_s)$ was calculated. Figure 12 shows the relationship between $CV(V_s)$ and the flow Froude number F for $d_{50} = 0.014$ mm (Figure 12a) and $d_{50} = 4.7$ mm (Figure 12b).

3.2 | Evaluating the correction factor for rill flows

Figure 13a (soil) and Figure 13b (gravel) show the (Re, α_v) pairs, with $\alpha_v = V/V_m$, for the two investigated measurement techniques and rough beds. This figure demonstrates that, in both cases, for the investigated turbulent channelized flows (2193 ≤ Re ≤ 8770 for d_{50} = 0.014 mm and 2713 ≤ Re ≤ 11 499 for d_{50} = 4.7 mm), α_v is independent of Re. The analysis also demonstrated that the correction factor α_v (=V/V_m) and the Froude number F_s are not correlated.

For each investigated slope value, the frequency distributions of $\alpha_v = V/V_s$ are plotted, as an example for the CB technique, in Figure 14 while the corresponding descriptive statistics for all the four technique-roughness combinations are listed in Table 3.

Figure 15, which shows the $s - \alpha_{vm}$ experimental pairs, highlights that α_{vm} and s are not correlated for both the measurements techniques and investigated roughness conditions.

Finally, in the light of absence of suitable α_v predictors, the mean value of α_v (=V/V_s) for each slope was calculated (Table 3). Also,
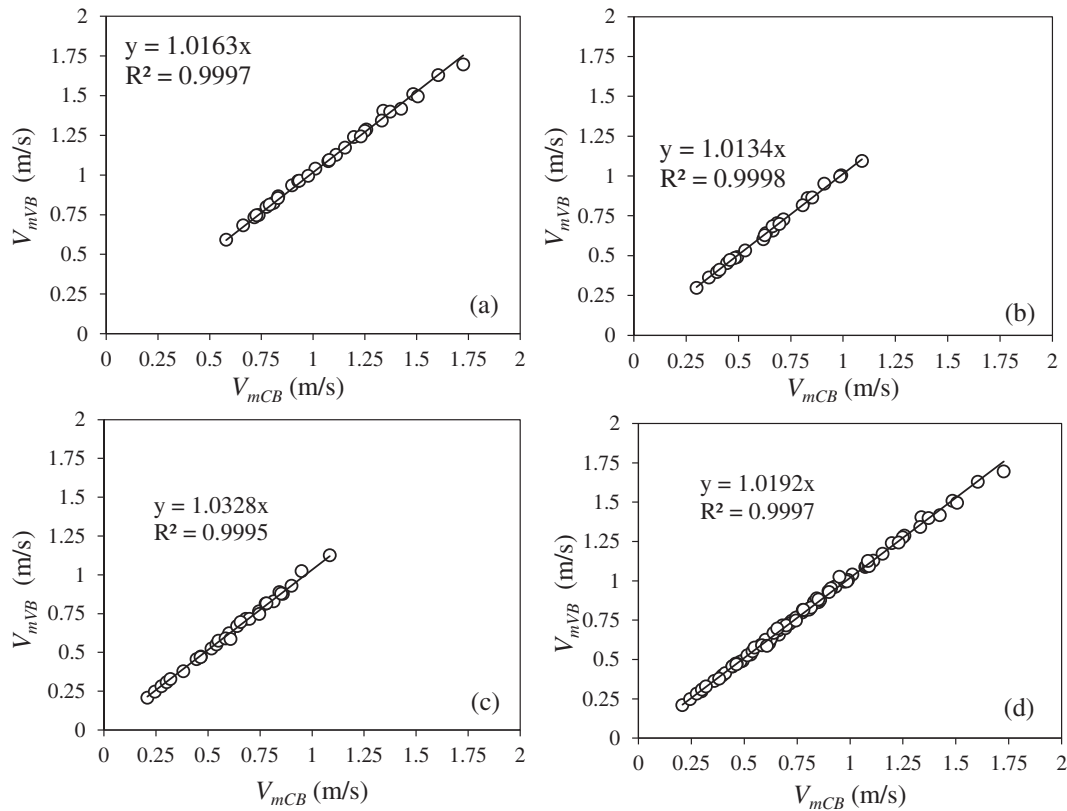
FIGURE 11 Comparison between the V_m values determined by VB and CB techniques for smooth (Di Stefano et al., 2021) (a), soil (b), gravel (c) case and all data (d)
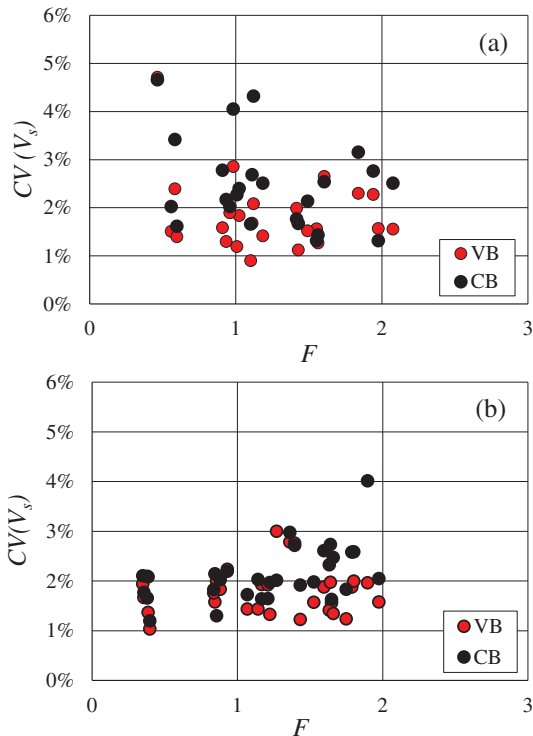

FIGURE 12 Relationship between F and $CV(V_s)$ for soil (a) and gravel (b) arrangement

assuming the hypothesis of slope-independence of α_v, the mean value of each whole dataset was calculated ($\alpha_v = 0.66$ (VB) and $\alpha_v = 0.67$ (CB) for $d_{50} = 0.014$ mm and $\alpha_v = 0.75$ (VB) and $\alpha_v = 0.77$ (CB) for $d_{50} = 4.7$ mm).

The statistics of the 480 (soil) or 600 (gravel) absolute errors on the estimate of the mean flow velocity, $|(\alpha_v V_s - V)/V|$, are listed in Table 4. Figure 16 shows, as an example for the CB technique, the frequency distributions of the relative errors. The latter, which are calculated as the difference between the forementioned mean values and the 480 (soil) or 600 (gravel) α_v normalized using these measurements, are normally distributed with a mean almost equal to zero for both the examined techniques and roughness conditions. The same result was obtained using the slope-specific α_v values.

4 | DISCUSSION

4.1 | Comparison between VB and CB technique for measuring surface flow velocity

The results shown in Figures 7, 8 and 9 agree with those obtained by Di Stefano et al. (2021) for experiments carried out on the same flume with smooth bed and walls ($d_{50} = 0$). These results demonstrated that, for the VB and CB technique, the distribution of the V_s/V_m ratio is
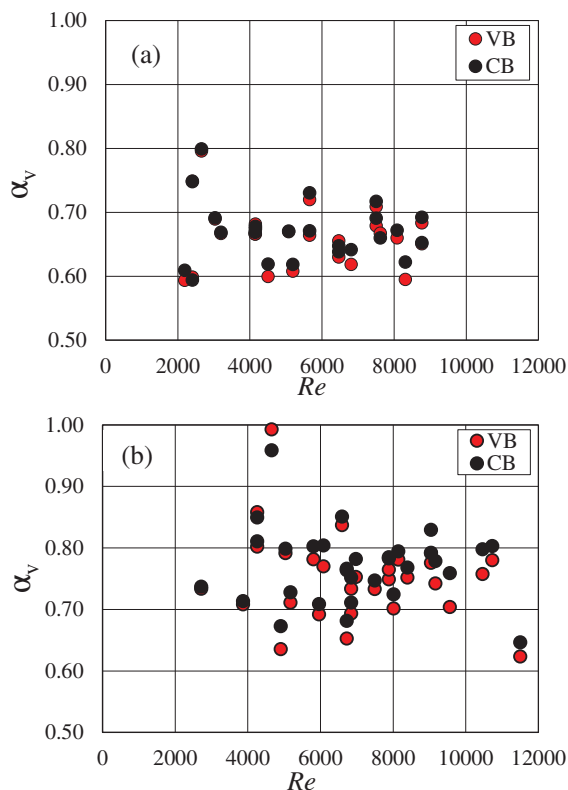
FIGURE 13 Relationship between Re and α_v for soil (a) and gravel (b) arrangement
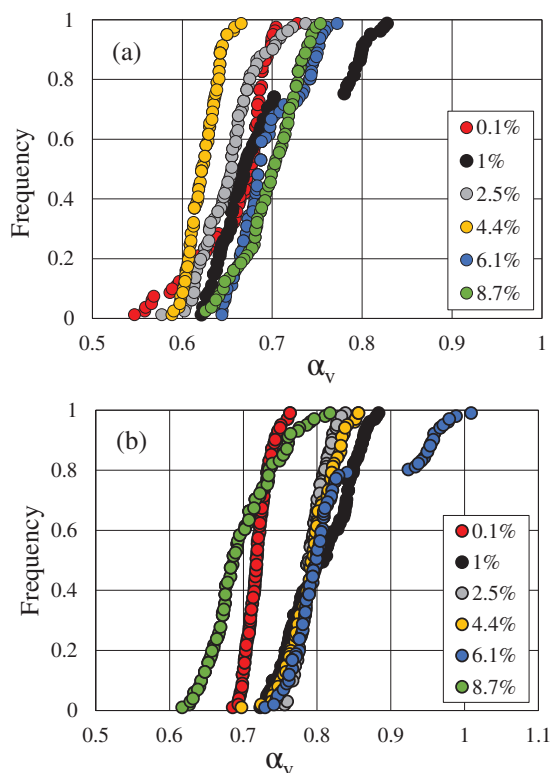

FIGURE 14 Empirical frequency distributions of α_v for each slope s, as an example for CB-soil (a) and CB-gravel (b) combinations

TABLE 3 Statistics of the ratio $\alpha_v = V/V_s$ for each investigated slope value

| Technique | s (%) | Soil | | | | |
		Min	Max	Mean	Median	CV
VB	0.1	0.543	0.699	0.654	0.667	0.0549
	1	0.643	0.810	0.700	0.673	0.0815
	2.5	0.577	0.720	0.641	0.643	0.0432
	4.4	0.575	0.634	0.602	0.600	0.0232
	6.1	0.637	0.775	0.691	0.678	0.0542
	8.7	0.623	0.735	0.692	0.697	0.0417
CB	0.1	0.547	0.728	0.658	0.675	0.0638
	1	0.621	0.828	0.694	0.668	0.0930
	2.5	0.577	0.737	0.652	0.655	0.0480
	4.4	0.588	0.666	0.623	0.622	0.0274
	6.1	0.644	0.772	0.695	0.687	0.0515
	8.7	0.626	0.754	0.698	0.702	0.0472
Technique	s (%)	Gravel				
		Min	Max	Mean	Median	CV
VB	0.1	0.664	0.762	0.708	0.704	0.0269
	1	0.707	0.889	0.792	0.779	0.0640
	2.5	0.722	0.830	0.763	0.760	0.0326
	4.4	0.690	0.848	0.768	0.765	0.0356
	6.1	0.740	1.019	0.819	0.781	0.1084
	8.7	0.604	0.741	0.664	0.658	0.0543
CB	0.1	0.686	0.763	0.720	0.718	0.0234
	1	0.723	0.883	0.804	0.808	0.0558
	2.5	0.755	0.838	0.792	0.789	0.0243
	4.4	0.697	0.856	0.793	0.793	0.0393
	6.1	0.729	1.009	0.823	0.799	0.0873
	8.7	0.617	0.817	0.697	0.687	0.0643

independent of slope and discharge, which means that the mean value V_m accounts for the effects of both slope and discharge on surface flow velocity.

The values of standard deviation of V_s/V_m show that, for both the roughness conditions, the variability of V_s/V_m is slightly lower for the VB technique as compared to the CB. Therefore, for a rough condition the two examined techniques have a comparable precision.

For the VB technique the variability of the V_s/V_m measurements for the rough condition is more relevant than that for the smooth condition while for the CB technique this variability is comparable with that of the smooth case. In other words, the precision of CB technique is independent of roughness while differences occur for the VB technique. The circumstance that the roughness elements cause a transversal dispersion of the dye (Figure 6b), due to the transversal component of the flow velocity, may cause some difficulties in detecting the dye front and the travel time, consequently. For the VB technique the detection of the dye front is the unique reason of
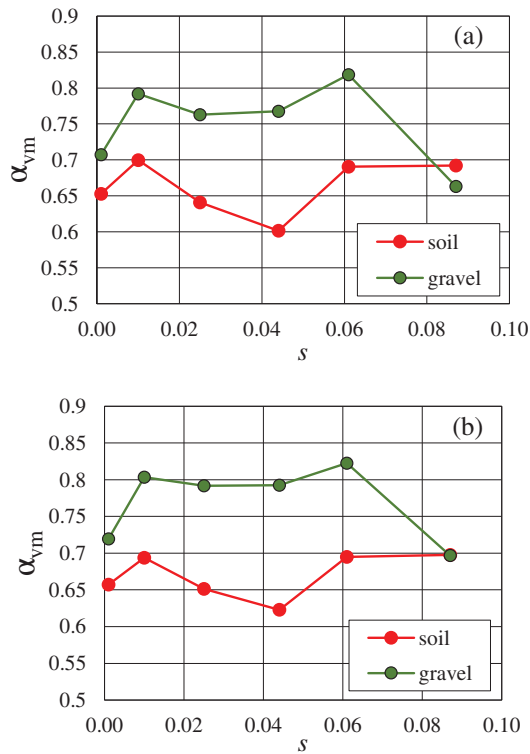
FIGURE 15 Relationship between the correction factor α_{vm} and slope s corresponding to the two roughness arrangements for VB (a) and CB (b) technique
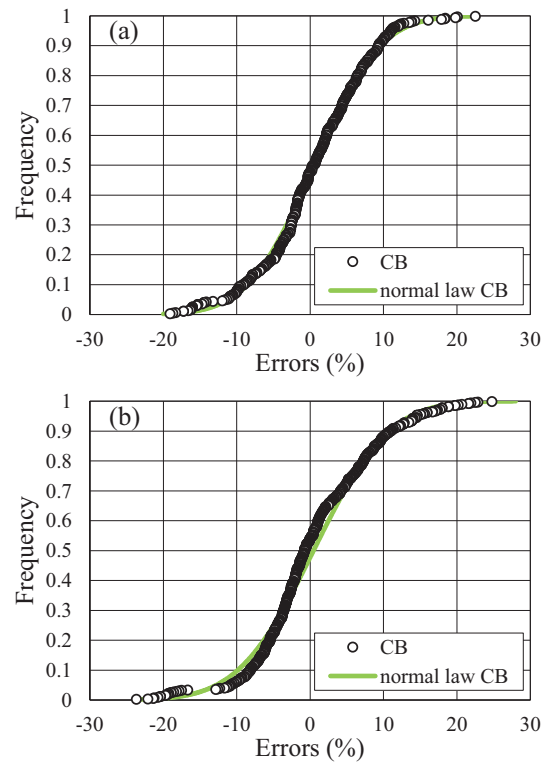

FIGURE 16 Examples of frequency distributions of the relative errors, calculated as the difference between the mean values of α_v and the α_v measurements normalized using these measurements, for CB-soil (a) and CB-gravel (b) combinations

TABLE 4 Absolute error values on the estimate of V

	Gravel-VB		Gravel-CB	
	([a])	([b])	([a])	([b])
Min	0.0365%	0.0135%	0.0089%	0.0193%
Max	19.7%	26.4%	18.4%	24.8%
Mean	4.3%	6.5%	3.9%	6.2%

	Soil-VB		Soil-CB	
	([a])	([b])	([a])	([b])
Min	0.04%	0.03%	0.009%	0.026%
Max	20.4%	21.5%	20.3%	22.5%
Mean	4.8%	5.7%	4.9%	5.6%

[a]Slope-specific α_v.
[b]α_v = constant.

measurement uncertainty, while for the CB technique the uncertainty due to dye dispersion also affects the reaction time of the operator. However, for the CB technique no substantial difference between the smooth and rough case was detected. Furthermore, the normal distribution of V_s/V_m fits well the empirical frequency distribution. This finding agrees with that obtained by Di Stefano et al. (2021) for the smooth flume case.

The present empirical frequency analysis and the results by Di Stefano et al. (2021) demonstrate that the mean $V_s/V_m = 1$ is

representative for both measurement techniques and the three examined values of d_{50} (0, 0.014, 4.7 mm) and therefore V_m can be used to compare the two different techniques.

Equations (3), (4) and (5) show that, for the three roughness conditions, the VB velocity measurement is on average greater than the CB one but of 3.3% at the most. Therefore, neglecting the differences among these equations, the following unique $V_{mCB} - V_{mVB}$ relationship was calibrated (Figure 11d):

$$V_{mVB} = 1.019 V_{mCB} \qquad (6)$$

with coefficient of determination equal to 0.998. This result confirms the reliability of the CB technique, which is, overall, less time-consuming as it does not require a video-analysis phase.

Figure 12a shows that CV(V_s), for the VB technique, does not depend on flow Froude number, varies mainly from 1% to 3% and is on average equal to 1.9% for $d_{50} = 0.014$ mm and 1.8% for $d_{50} = 4.7$ mm. For the CB technique (Figure 12b), CV(V_s) does not depend on flow Froude number and varies mainly from 1% to 3%, even if there are five values greater than 3% for $d_{50} = 0.014$ mm and a single value greater than 3% for $d_{50} = 4.7$ mm. In this case, CV(V_s) is on average equal to 2.5% for $d_{50} = 0.014$ mm and 2.1% for $d_{50} = 4.7$ mm. In any case, for a fixed F value a low variability of the 20 measurements of V_s around the mean V_m occurs. This
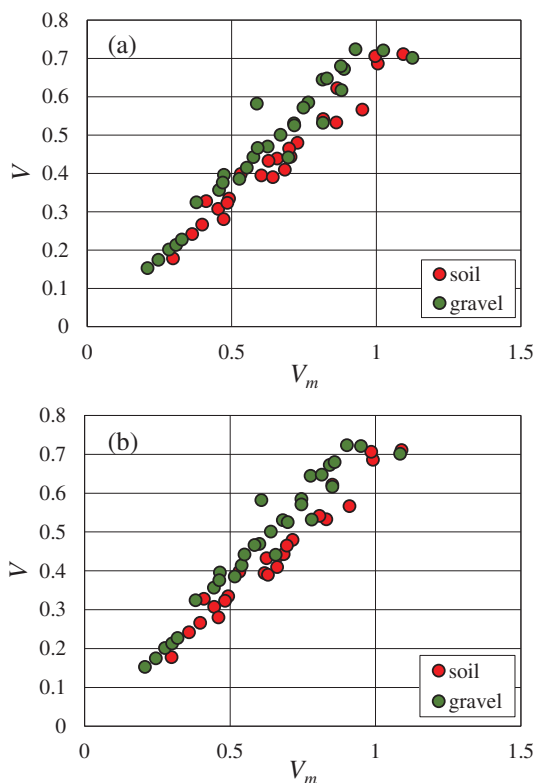
FIGURE 17 Comparison between mean flow velocity V and mean surface flow velocity V_m for VB (a) and CB (b) technique

FIGURE 18 Frequency distribution of the Strickler coefficient c for both the investigated roughness conditions

result confirms the measurement reliability for both the roughness conditions and measurement techniques.

4.2 | Evaluating the correction factor for rill flows

The result shown in Figure 13 confirms that the correction factor is not influenced by Re, as already demonstrated by Di Stefano et al. (2021) for turbulent channelized flows on a smooth flume. For turbulent flows, the eddy mixing ensures that the surface velocity exceeds the mean velocity by a lesser amount compared to laminar flow (Dunkerley, 2001). In addition, the magnitude of this mixing effect does not seem to substantially affect the flow velocity profile, resulting in correction factors not significantly varying with Re. The same results were obtained for turbulent overland (Li & Abrahams, 1997) flows.

The analysis of the $\alpha_v = V/V_s$ values (Figure 14) obtained with both techniques shows that the curves generally do not overlap, demonstrating the influence of the slope on the correction factor. Figure 14 and Table 3 show that, generally, both the α_v range and its variability expressed in terms of CV depend on the slope. However, for both the measurements techniques and investigated roughness conditions, α_{vm} and s are not correlated (Figure 15). Except for $s = 8.7\%$, α_{vm} values for the gravel arrangement are higher than those obtained for the soil arrangement. This result can be justified by the circumstance that the water depth measurement for the highest slope
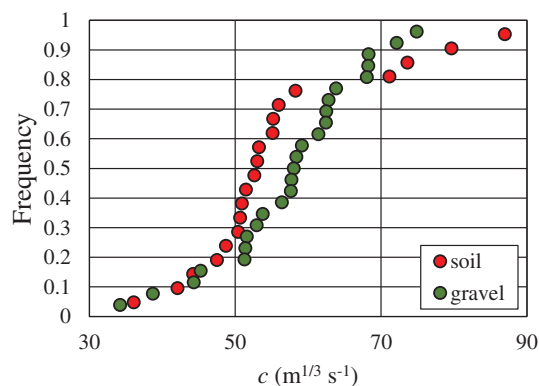
value ($s = 8.7\%$) is more affected by water surface irregularities than the measurement performed on the lower slopes.

For fixed mean surface velocity V_m and both the measurement techniques, the gravel arrangement is characterized by values of mean flow velocity V higher than those corresponding to the soil arrangement (Figure 17a,b). Figure 18, which shows the frequency distribution of the Strickler coefficient c ($m^{1/3}$ s^{-1}) for both soil and gravel arrangement, highlights that the c median value (53 $m^{1/3}$ s^{-1}) of the soil is lower than that (58 $m^{1/3}$ s^{-1}) of the gravel. In other words, the gravel was hydraulically smoother than the soil. This last result justifies that the gravel is characterized by values of α_v (Figure 15a,b) and V (Figure 17a,b) higher than those of the soil.

The circumstance that the gravel arrangement is smoother than the soil one can originate from the deployment of gravel particles, which are oriented with the smallest or intermediate dimension perpendicular to the flume bed and walls.

Table 4 shows that using a constant value of α_v gives a worse estimate of V compared to that yielded using the slope-specific α_v value, especially for the case of flume covered with gravel. However, using a constant α_v for each investigated roughness condition, the errors are randomly distributed around zero (Figure 16) and it can be considered representative of the correction factor, accordingly.

Finally, being the mean estimate errors of mean flow velocity relatively low, dye-tracing can be considered a simple and reliable measurement method.

5 | CONCLUSIONS

The applicability of the dye-tracer technique needs an appropriate correction factor α_v for different hydraulic and bed conditions to scale down the measured surface velocity V_s. In this paper, experiments were performed to study the applicability of the dye-tracer technique in a small channel simulating a rill. Two techniques for measuring the travel time of the dye-tracer and two roughness conditions were used.

The analysis allowed to establish the following main results:

i. for both investigated measurement techniques and rough beds, a single surface velocity measurement is, on average, representative of this kinetic variable;

ii. the mean value V_m of the surface flow velocity, which is representative of the scale effect due to the discharge and slope, can be used to compare the two examined measurement techniques for $0 \leq d_{50} \leq 4.7$ mm;

iii. for the examined rough flumes both the measurement techniques allow precise surface flow velocity measurements.

Furthermore, in accordance with previous results obtained with the same flume for the smooth bed condition, the developed analysis on the correction factor confirmed that α_v is not correlated with Reynolds number for turbulent flow regime. The results also demonstrated that the correction factor is not correlated with the Froude number F_s and the channel slope. However, the analysis of the empirical frequency distributions led to recognize a slope effect on the correction factor.

DATA AVAILABILITY STATEMENT

The data that support the findings of this study are available on request from the corresponding author.

ORCID

Alessio Nicosia https://orcid.org/0000-0003-0540-8788
Vincenzo Palmeri https://orcid.org/0000-0001-6594-9530
Vincenzo Pampalone https://orcid.org/0000-0002-5195-9209
Vito Ferro https://orcid.org/0000-0003-3020-3119

REFERENCES

Abrahams, A. D., Li, G., & Parsons, A. J. (1996). Rill hydraulics on a semiarid hillslope, southern Arizona. *Earth Surface Processes and Landforms*, *21*, 35–47.

Ali, M., Sterk, G., Seeger, M., & Stroosnijder, L. (2012). Effect of flow discharge and median grain size on mean flow velocity under overland flow. *Journal of Hydrology*, *452-453*, 150–160.

Ayala, J. E., Martinez-Austria, P., Menendez, J. R., & Segura, F. A. (2000). Fixed bed forms laboratory channel flow analysis. *Ingenieria Hidraulica ex Mexico*, *15*(2), 75–84.

Bagarello, V., Di Stefano, C., Ferro, V., & Pampalone, V. (2015). Establishing a soil loss threshold for limiting rilling. *Journal of Hydrologic Engineering, ASCE*, *20*(C6014001), 1–5.

Ban, Y., Lei, T., Liu, Z., & Chen, C. (2016). Comparison of rill flow velocity and thawed slopes with electrolyte tracer method. *Journal of Hydrology*, *534*, 630–637.

Berman, E. S. F., Gupta, M., Gabrielli, C., Garland, T., & McDonnell, J. J. (2009). High-frequency field deployable isotope analyzer for hydrological applications. *Water Resources Research*, *45*(W10201), 1–7.

Bradley, A. A., Kruger, A., Meselhe, E. A., & Muste, M. V. (2002). Flow measurement in streams using video imagery. *Water Resources Research*, *38*(12), 1315, 51-1–51-8.

Bruno, C., Di Stefano, C., & Ferro, V. (2008). Field investigation on rilling in the experimental Sparacia area, South Italy. *Earth Surface Processes and Landforms*, *33*, 263–279.

Chen, C., Ban, Y., Wang, X., & Lei, T. (2017). Measuring flow velocity on frozen and non-frozen slopes of black soil through leading edge method. *International Soil and Water Conservation Research*, *5*, 180–189.

Coleman, N. L. (1986). Effects of suspended sediment on the open—Channel velocity distribution. *Water Resources Research*, *22*, 1377–1384.

de Lima, J. L. M. P., & Abrantes, J. R. C. B. (2014). Using a thermal tracer to estimate overland and rill flow velocities. *Earth Surface Processes and Landforms*, *39*, 1293–1300.

Di Stefano, C., Ferro, V., & Pampalone, V. (2015). Modeling rill erosion at the Sparacia experimental area. *Journal of Hydrologic Engineering, ASCE*, *20*(C5014001), 1–12.

Di Stefano, C., Ferro, V., Palmeri, V., & Pampalone, V. (2017a). Measuring rill erosion using structure from motion: A plot experiment. *Catena*, *153*, 383–392.

Di Stefano, C., Ferro, V., Palmeri, V., & Pampalone, V. (2017b). Flow resistance equation for rills. *Hydrological Processes*, *31*, 2793–2801.

Di Stefano, C., Ferro, V., Palmeri, V., & Pampalone, V. (2018a). Testing slope effect on flow resistance equation for mobile bed rills. *Hydrological Processes*, *32*, 664–671.

Di Stefano, C., Ferro, V., Palmeri, V., & Pampalone, V. (2018b). Assessing dye-tracer technique for rill flow velocity measurements. *Catena*, *171*, 523–532.

Di Stefano, C., Nicosia, A., Palmeri, V., Pampalone, V., & Ferro, V. (2020). Dye-tracer technique for rill flows by velocity profile measurements. *Catena*, *185*(104313), 1–7.

Di Stefano, C., Nicosia, A., Palmeri, V., Pampalone, V., & Ferro, V. (2021). Flume experiments for assessing the dye-tracing technique in rill flows. *Flow Measurement and Instrumentation*, *77*(2), 101870.

Dunkerley, D. L. (2001). Estimating the mean speed of laminar overland flow using dye injection-uncertainty on rough surfaces. *Earth Surface Processes and Landforms*, *26*, 363–374.

Dunkerley, D. L. (2003). An optical tachometer for short-path measurement of flow speeds in shallow overland flows: Improved alternative to dye timing. *Earth Surface Processes and Landforms*, *28*, 777–786.

Emmett, W. W.. (1970). The hydraulics of overland flow on hillslopes. U.S. Geological Survey Professional Papers 622-A.

Ferro, V., & Baiamonte, G. (1994). Flow velocity profiles in gravel-bed rivers. *Journal of Hydraulic Engineering, ASCE*, *120*(1), 60–80.

Ferro, V. (2003). Flow resistance in gravel-bed channels with large-scale roughness. *Earth Surface Processes and Landforms*, *28*(12), 1325–1339.

Foster, G. R., Huggins, L. F., & Meyer, L. D. (1984). A laboratory study of rill hydraulics: I. Velocity relationships. *Transactions of the ASAE*, *27*, 790–796.

Gilley, J. E., Kottwitz, E. R., & Simanton, J. R. (1990). Hydraulics characteristics of rills. *Transaction of the ASAE*, *27*, 797–804.

Giménez, R., Planchon, O., Silvera, N., & Govers, G. (2004). Longitudinal velocity patterns and bed morphology intercation in a rill. *Earth Surface Processes and Landforms*, *29*, 105–114.

Govers, G. (1992). Relationship between discharge, velocity and flow area for rills eroding loose, non-layered materials. *Earth Surface Processes and Landforms*, *17*, 515–528.

Horton, R. E., Leach, H. R., & Vliet, V. R. (1934). Laminar sheet flow. *Transactions of the American Geophysical Union*, *15*, 393–404.

Kirkman, T. W. (1996). *Statistics to use*. http://www.physics.csbsju.edu/stats/1996 (July 2021).

Lei, T., Xia, W., Zhao, J., Liu, Z., & Zhang, Q. (2005). Method for measuring velocity of shallow water flow for soil erosion with an electrolyte tracer. *Journal of Hydrology*, *301*, 139–145.

Li, G., Abrahams, A. D., & Atkinson, J. F. (1996). Correction factors in the determination of mean flow velocity of overland flow. *Earth Surface Processes and Landforms*, *21*, 509–515.

Li, G., & Abrahams, A. D. (1997). Effect of salting sediment load on the determination of the mean velocity of overland flow. *Water Resources Research*, *33*, 341–347.

Line, D. E., & Meyer, L. D. (1988). Flow velocities of concentrated runoff along cropland furrows. *Transactions of the ASAE*, *31*, 1435–1439.

Liu, Z., Adrian, R. J., & Hanratty, T. J. (2001). Large-scale modes of turbulent channel flow: Transport and structure. *Journal of Fluid Mechanics*, *448*, 53–80.

Luk, S. H., & Merz, W. (1992). Use of the salt tracing technique to determine the velocity of overland flow. *Soil Technology*, *5*, 289–301.

Novak, G., Rak, G., Prešeren, T., & Bajcar, T. (2017). Non-intrusive measurements of shallow water discharge. *Flow Measurement and Instrumentation*, *56*, 14–17.

Olivier, P., Norbert, S., Raphael, G., David, F. M., Wainwright, J., Le Bissonnais, Y., & Govers, G. (2005). An automated salt-tracing gauge for flow-velocity measurements. *Earth Surface Processes and Landforms*, *30*, 833–844.

Pan, C., Shangguan, Z., & Ma, L. (2015). Assessing the dye-tracer correction factor for documenting the mean velocity of sheet flow over smooth and grassed surfaces. *Hydrological Processes*, *29*, 5369–5382.

Planchon, O., Silvera, N., Giménez, R., Favis-Mortlock, D., Wainwright, J., Le Bissonnais, Y., & Govers, G. (2005). An automated salt-tracing gauge for flow-velocity measurement. *Earth Surface Processes and Landforms*, *30*, 833–844.

Polyakov, V., Li, L., & Nearing, M. A. (2021). Correction factor for measuring mean overland flow velocities on stony surfaces under rainfall using dye tracer. *Geoderma*, *390*, 114975.

Powell, D. M. (2014). Flow resistance in gravel-bed rivers: Progress in research. *Earth-Science Reviews*, *136*, 301–338.

Raffel, M., Willert, C., & Kompnhans, J. (1998). Particle image velocimetry. In *A Practical Guide (Experimental Fluid Mechanics)*. Springer.

Takken, I., Govers, G., Ciesiolka, C. A. A., Silburn, D. M., & Loch, R. J. (1998). *Factors influencing the velocity-discharge relationship in rills. Modelling soil erosion, sediment transport and closely related hydrological processes* (pp. 63–69). IAHS Publ. N. 249.

Ventura, E., Jr., Nearing, M. A., & Norton, L. D. (2001). Developing a magnetic tracer to study soil erosion. *Catena*, *43*, 277–291.

Wirtz, S., Seeger, M., & Ries, J. B. (2010). The rill experiment as a method to approach a quantification of rill erosion process activity. *Zeitschrift für Geomorphologie*, *54*, 47–64.

Wirtz, S., Seeger, M., & Ries, J. B. (2012). Field experiment for understanding and quantification of rill erosion processes. *Catena*, *91*, 21–34.

Yang, D. M., Fang, N. F., & Shi, Z. H. (2020). Correction factor for rill flow velocity measured by the dye tracer method under varying rill morphologies and hydraulic characteristics. *Journal of Hydrology*, *591*, 125560.

Zhang, G., Luo, R., Cao, Y., Shen, R., & Zhang, X. C. (2010). Correction factor to dye-measured flow velocity under varying water and sediment discharges. *Journal of Hydrology*, *389*, 205–213.